

JOURNAL OF ADVANCED APPLIED SCIENCES

e-ISSN: 2979-9759



RESEARCH ARTICLE

Non-Destructive Testing Using Transmission Line-Based Microwave Sensors

Sanam Movazzafgharehbagh[™] • Faruk Karadağ •

Çukurova University, Faculty of Science, Department of Physics, Adana/Türkiye

ARTICLE INFO

Article History

Received: 31.10.2023 Accepted: 07.12.2023 First Published: 18.12.2023

Keywords

Concrete Metamaterial Sea sand Sensor



ABSTRACT

In this study, some types of antennas and metamaterial structures have been designed and produced with the aim of determining and detecting ionized chlorine of sea sand in concrete. The first structure has a Loop-like resonator with the sample, the second structure has a Bowtie-shaped resonator with the sample and the third structure has double loop resonators on both sides of concrete samples also non-destructive method is applied for all structures. Different samples of concrete are produced with different proportions of ionized sea sand. Electrical properties of concrete samples for all structures are investigated in the frequency range of 1-9 GHz. The structures are designed in the CST Microwave Studio program. Also, the simulation study of the designed structures shows that the most important resonance frequency changes, considering the dielectric constant of concrete samples, for the Loop-like structure occur in the 1-8 GHz, Bowtie-shaped structure in 1-4 GHz and double Loop structure in 1-9 GHz of frequency band. The important point in this study is the changes of the waveform at the resonance frequency. The output waveform (reflection coefficient S11/transmission coefficient S12) should change in linear form by considering the dielectric coefficient. We have used copper for the resonators and also the material with & value of 3 as the substrate layers of the structures. We have simulated three types of designed structures with CST Microwave Software and then achieve the results and evaluate them. Both numerical and experimental tests have given approximately same results and are in good agreement with each other. These proposed structures can be used in many applications where it is necessary to determine the rate of ionized sea sand in cement-based composites such as concrete.

Please cite this paper as follows:

Movazzafgharehbagh, S., & Karadağ, F. (2023). Non-destructive testing using transmission line-based microwave sensors. *Journal of Advanced Applied Sciences*, 2(2), 73-82. https://doi.org/10.61326/jaasci.v2i2.109

1. Introduction

Metamaterials (MTMs) are materials that manufactured, created, or constructed by human beings specifically. These materials are an arrangement of metal pieces on a special substrate for standard and suitable performance at the desired microwave frequency range. MTMs have extraordinary and unusual features such as negative refraction, doppler effect and so on (Veselago, 1968; Plum et al., 2009; Liu et al., 2015). These materials with unusual electromagnetic properties (MTMs) theoretically proposed by the Russian physicist Viktor

Veselago in 1968 (Veselago, 1968). After Victor Veselago's paper or proposal in 1967, more than 30 years elapsed by trying the group of researchers in 2000, the first MTM was developed artificially with negative permeability and negative permittivity by using periodic metal resonators therefore at the end of the 20th century, first MTM exhibit as expected by Veselago, and then MTMs were fabricated and began to be used in practical life with the help of Pendry et al. (1996, 1999) and Smith et al. (2000). MTMs are used in sensing applications because of their different features such as energy harvesting applications, signal absorbers, shielding, cloaking and many other sectors (Cai et

E-mail address: sanam.mov61@gmail.com



[™] Correspondence

al., 2007; Zhang et al., 2009; Bakır et al., 2018a, 2019; Abdulkarim et al., 2019; Zile, 2019). Sensing structures based on electromagnetic materials have become newly accessible and accepted for use in many fields (Abbas et al., 2005; L. Yang et al., 2011; Chieh-Sen & Yang, 2014; C. L. Yang et al., 2016). Different scientists and research teams have developed applications of microwave sensors at the liquid or solids materials due to the severe limitation and focus on a specific point of electromagnetic fields. MTM sensors are capable of sensing solids (Akgol & Unal, 2018). MTM microwave sensors have advantages or, on the contrary, along with these advantages, they also have disadvantages. Some microwave sensors such as the microfluidic sensor have best and optimized quality in sensor applications (Bakır, 2017) and some of them may be economical, cheap with high detection and sensing (Bakır et al., 2018b). A fundamental behavior and basic action that we apply in MTM sensing applications is introduce the complex dielectric constant and include them, after that, we observe its effect in the form of resonance frequency changes. In some structures, for high and optimized sensing split ring resonators (SRR) are used on both sides or in the middle of the sensor (Ebrahimi et al., 2014). Concrete is chosen as a building material for numerical, simulation and experimental work because concrete is a brittle material that provides less resistance to tensile stress. Today, reinforced concrete is used in many structures especially engineering structures and many ways have been proposed with many components and materials to increase the strength of cement-based composites to increase their useful life. The amount of additives such as sea sand in concrete samples can cause the formation of weak or strong concrete. The change of resonance frequency and magnitude of reflection (S₁₁) and transmission coefficients (S₁₂) which are related to the permeability (E) of concrete enables us to determine the characteristics of chlorinated sea in cement based materials, so the aim of this study is investigating and determining the effect of ionized chlorine sea sand on concrete by Non-destructive testing.

2. Materials and Methods

2.1. Process of Making Ionised Concrete Samples

The ingredients and materials for preparing the building concrete samples were Portland cement (CEM 42.5R), crushed aggregates, sea sand and tap water. The weight and specific weight of finely crushed aggregate was 2.6 and the weight and specific weight of sea sand was 2.7, both of them had a maximum granularity of 4 mm, and also the physical characteristics of the materials are also shown in Table 1. Five different concrete mortar mixtures are prepared, which are explained in more detail below. In order to compare the EM properties with reflection/transmission (S11/S12) coefficients of ionized sea sand ones, a control sample was prepared by including natural fine aggregate, cement and water. Four other

different concrete mortars with different ionized sea sand contents with rate of 25%, 50%, 75% and 100% were prepared.

Table 1. Physical properties of the materials.

	Specific Gravity	Maximum Grain Size (mm)
Crushed fine aggregate	2.6	4
Sea sand	2.7	4

2.2. Mix Proportions of the Material Under Test with Different Sea Sand Contents

All concrete samples as seen in Figure 1, had a fixed ratio of cement: aggregate: water as 1:2.47:0.485, which occurred continuously in a production period. The samples were prepared with the above materials and one of them was prepared without using sea sand and the rest was prepared by replacing sea sand with finely crushed aggregates in the concrete samples. First, we mixed dry aggregate and dry cement then we added water and mixed it again. Mixing the ingredients continued to get a smooth and uniform mixture. In order to produce cementitious samples, we have poured the mentioned stir into cylindrical shaped containers with a diameter of 10 cm and a height of 5 cm, and after about a day we removed the composites from their molds.



Figure 1. Shapes of concrete samples.

2.3. Dielectric Measurements of Ionised Concrete Samples

Simulation studies are performed before the structures are built, so for this reason first the dielectric constant and loss factor of the material under test should be measured and loaded into simulation program that shown in Figure 2. Chlorine ratio in sea sand is different among the concrete samples. Each concrete sample was prepared with chlorine ratio of 0%, 25%, 50%, 75%, and 100% according to concrete volume. We paid attention to the mixing ratios and blending proportions to form

and create the concrete samples. The measurement procedure for dielectric of concrete samples was achieved by using probe kit with measurement software. Measurements were performed at the frequency of 1 GHz to 8 GHz, in our microwave laboratory. Five concrete samples with different proportions of chlorinated sea sand were measured. It is seen that the frequency band between 1 GHz and 8 GHz can be used and it is suitable for defining the chlorine ratios of sea sand on concrete with regard to the dielectric constant.

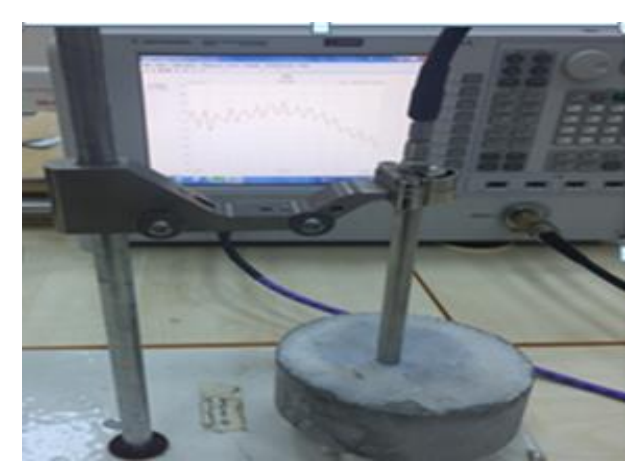


Figure 2. Measurement of dielectric values of concrete samples.

3. Results

3.1. Simulation Studies, Design of Antennas and Structures

Different structures have been designed in this study. The first design for cement-based materials, consists of a Loop-like resonator located in front of the substrate as presented in Figure 3. In the first structure, a micro sensor based on a Loop like shape resonator and in the other one Bow tie shaped resonator, were used to determine ratio of chlorine sea sand and effect of it in construction materials like concrete. In Figures 3 and 4, perspective views of the structures and the location of the sensing layer are demonstrated, with Cartesian coordinates and one discrete port is defined on board of two antennas.

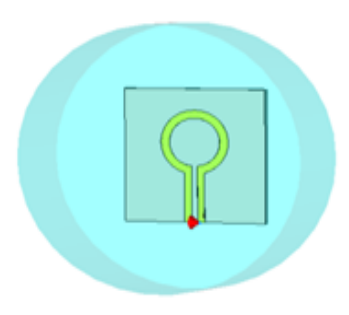


Figure 3. Perspective view of first structure (loop like shape structure).

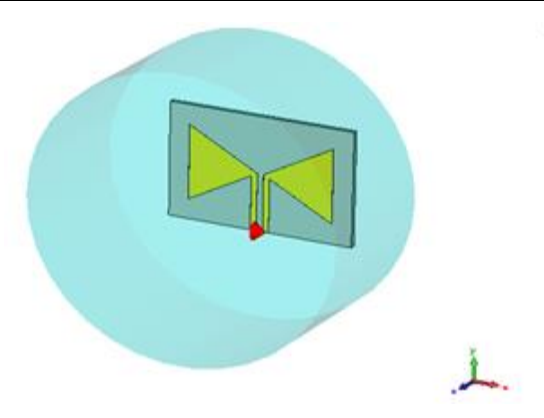


Figure 4. Perspective View of second structure (bow-tie shape structure).

For the third structure we have used two Loop antennas with two discrete ports that placed at two side of the concrete sample like Figure 5. Also, for measuring transmission coefficients, the fourth structure has designed like Figure 6. At first, we decided to design sensing layer with FR-4 but it was not available at that time in the lab so for the three structures we had to choose the material with Epsilon value of 3 which has got low loss specifications in the microwave frequency range. This substrate has 1.524 mm thickness to provide a strong signal feature and 1 magnetic permeability. Dimensions and thicknesses are determined and modeled using parametric studies to visualize and optimize dielectric constant changes placed near the Loop shaped and Bowtie shaped resonators. When designing this model, first the expected outputs are presented, and then the dimensions of the structure are determined in the operating frequency band with the CST Microwave Studio Program. After determining these dimensions, the resonator geometry is determined and after the geometry is determined, the design is completed by determining which results are close to the desired results. While the structure is designed, the present studies have been reviewed to adjust size and thicknesses of resonator and substrate according to the operating frequency. The best dimensions have been determined where the sensor capability is in good situation and therefore the production and testing steps have been carried out. The dimensions of the antenna and structure have been carefully selected to reduce measurement errors. For the fourth structure we choose FR-4 material as substrate with the thickness of 1.6 mm. Resonators can ampilfy mutual capacitance and inductance values. For all structures, resonators have thickness of 0.035 mm, made of copper and have conductivity of 5.8 x 106 S/m. Of course, we could have selected other dielectrics for the proposed structure, such as Rogers RT/ FR4/ Duroid laminates, and although these materials have lower losses in the microwave range but they are high-cost for construction applications. After measuring the complex dielectric constant values, these values were loaded into the CST Microsoft program operating with the finite integrated technique (FIT), and then cylindrical cementious samples with a diameter of 10 cm and a height of 5 cm were provided for numerical and simulation studies. As a result, these antennas are used as microwave sensors to identify ionized sea sand in concrete samples, which is dangerous in the construction industry.

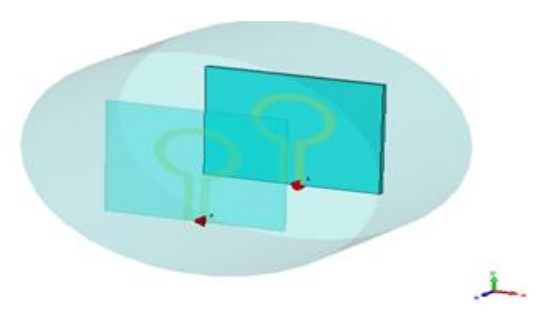


Figure 5. Perspective view of structure with two loop like antennas (third structure).

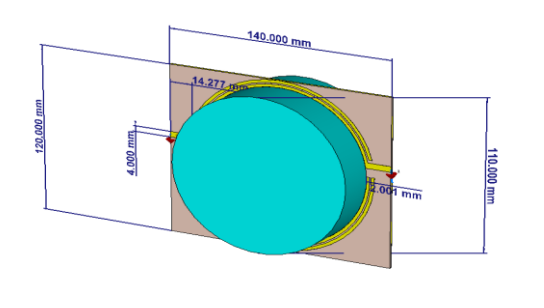
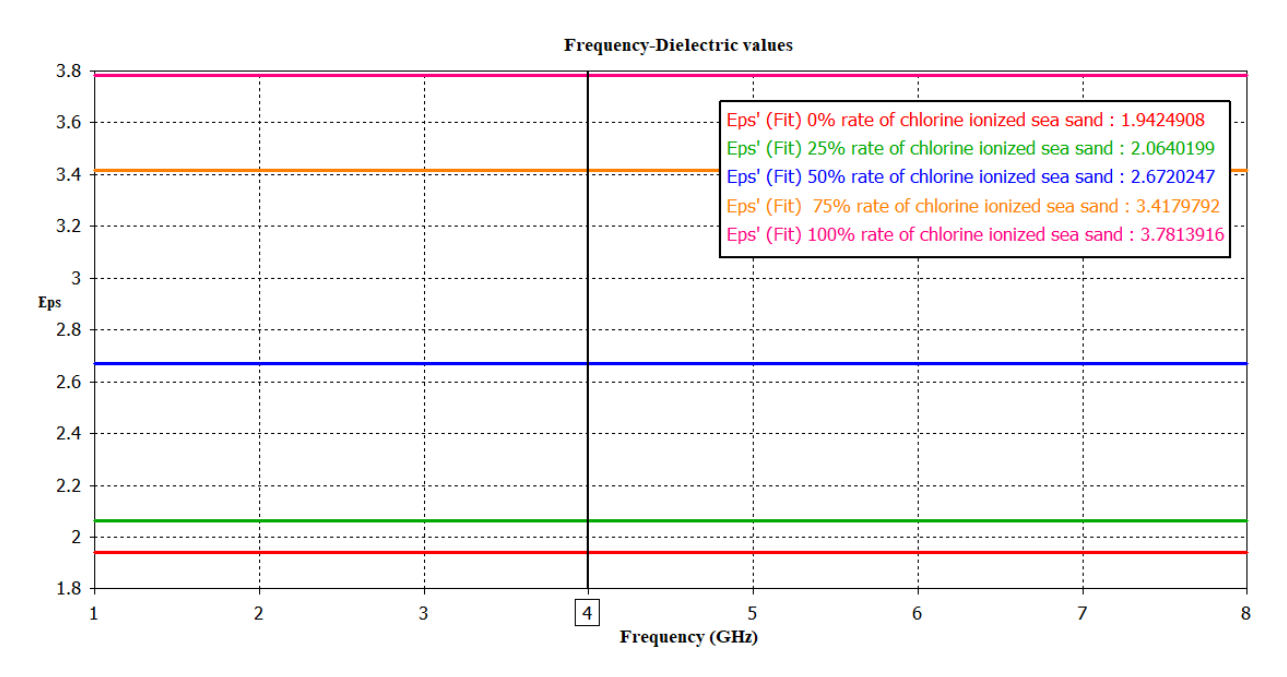


Figure 6. Perspective view of fourth structure.

3.2. Imputing Dielectric Constant of the Samples and Understanding of Numerical Simulations

Dielectric constant of five different samples including real part and imaginary part, called complex dielectric constant, measured in free space with Agilent PNA-L network analyzer and related graph is shown in Figure 7. It is seen that the dielectric constant value of each concrete sample is linear and increases, as the ratio of chlorine ionized sea sands in material increases. The measured composites samples have got sea sand with the content of 0, 25, 50, 75 and 100 percent. Considerable difference can be seen between the dielectric values of five concrete samples. It is seen that the increment of the rate of chlorine containing sea sand of the concrete increases the dielectric constant of the concrete. The dielectric constants of the samples are also evaluated in the same frequency band. Dielectric constants of chlorine sea sand in a concrete with ratios of 0%, 25%, 50%, 75%, and 100% were measured; it is shown in Figure 7. The concrete sample without sea sand (0%) has a dielectric value of around 1.94 in the frequency band and also according to the changes in the electrical quality or the characteristics of the samples by ionized particles that cause different dielectric constant values, the concrete samples with the proportion of 25%, 50%, 75%, and 100% sea sand, have 2.06, 2.95, 3.41, and 3.78 dielectric constant values, respectively.



Ĺ.

Figure 7. Dielectric constant of different chlorinated sea sand containing concretes.

Current flowing in the resonators can cause a magnetic field and then also cause the changes of the material under test (MUT) that placed as a building material. As the electrical properties in the resonator and port changes, the reflection/transmission coefficient (S11/S21) is consequently affected by these changes. The increase or decrease in the

volume of ionized sea sand content in concrete mortar, changed and shifted the resonance frequency due to reflection characteristic of the concrete samples with incident wave. In other words, the reflection/transmission responses due to polarization of the samples with their dielectricity constants for incident wave causes the resonance shifts. The simulated reflection/transmission coefficients (S11/S12) results are demonstrated in Figures 8-11. It is understood from the figures

that changing of dielectric constant influence the resonant frequency also change and create linear backward shifts.

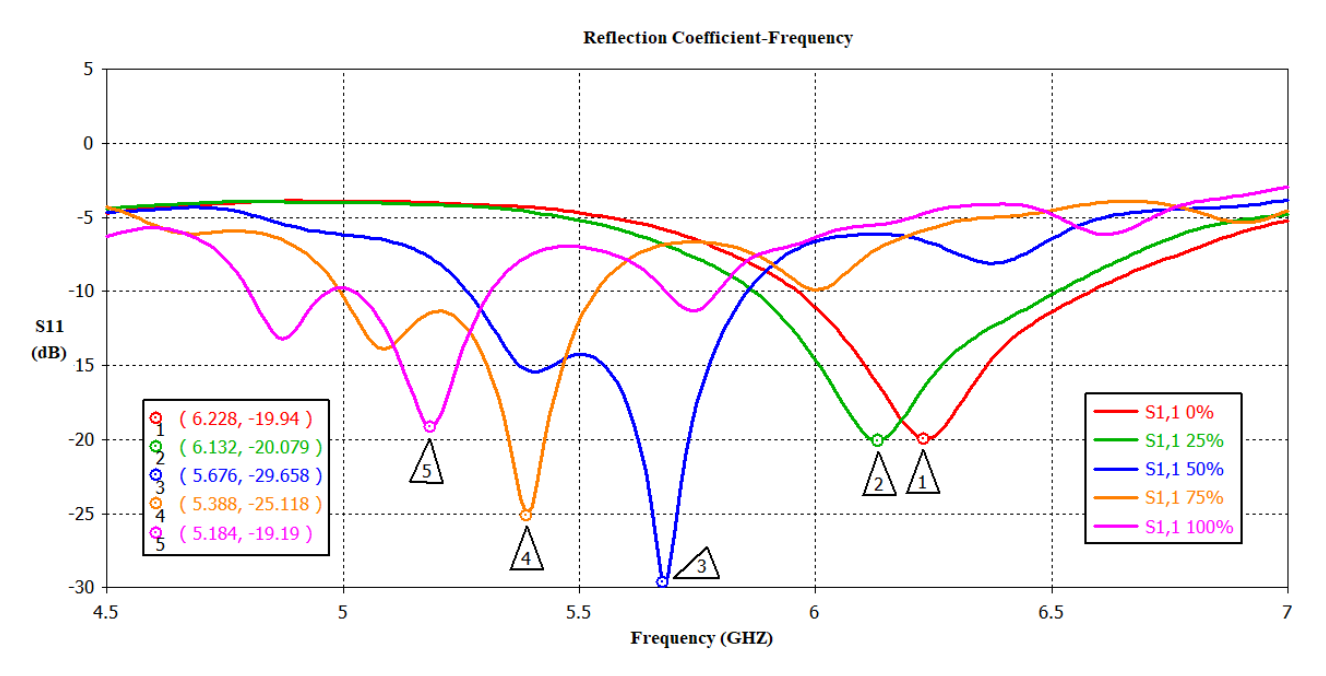


Figure 8. Simulation and reflection coefficient results (S11) results with various contents for first structure.

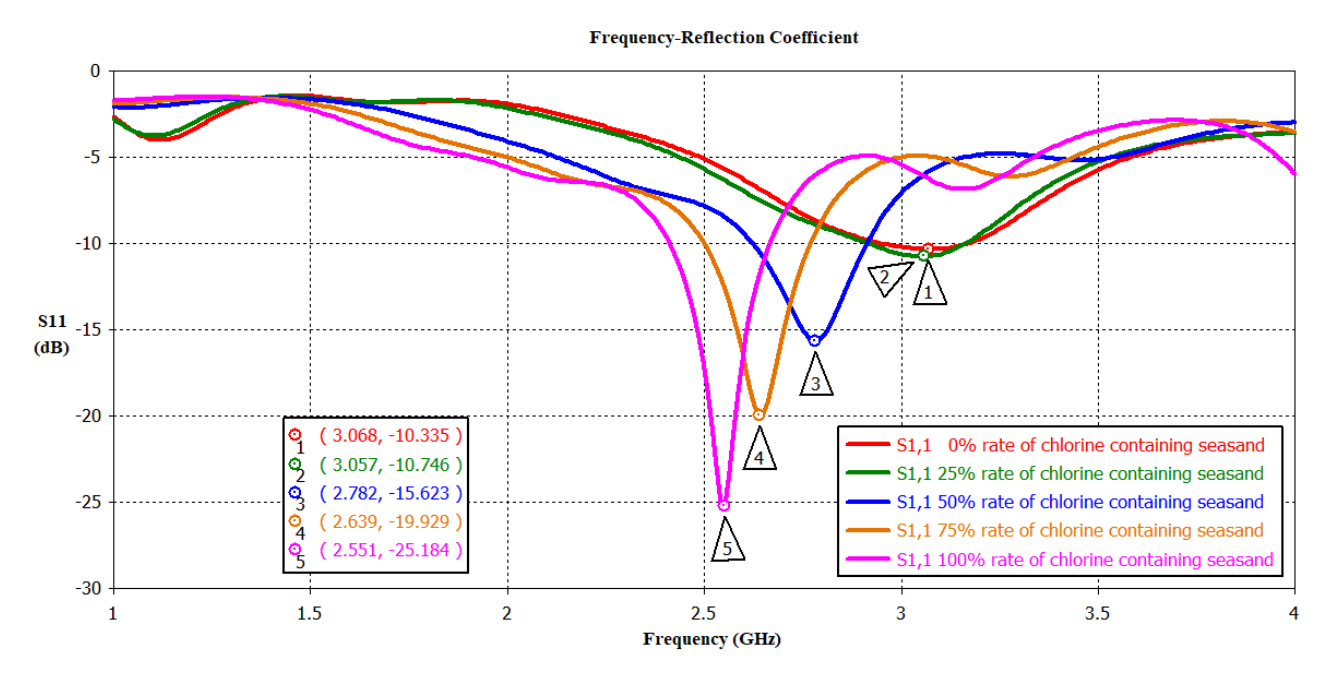


Figure 9. Simulation and reflection coefficient results (S11) results with various contents for second structure.

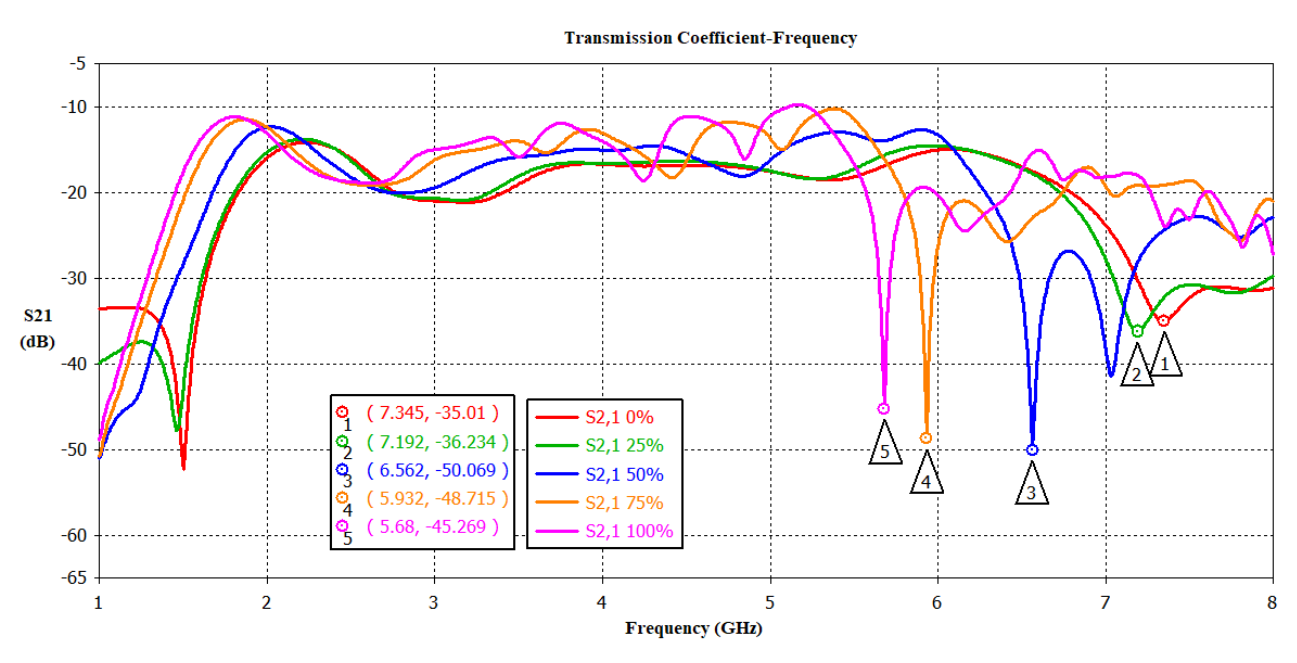


Figure 10. Simulation results and transmission coefficient results (S21) results with various contents for the structure with two loop like antennas (third structure).

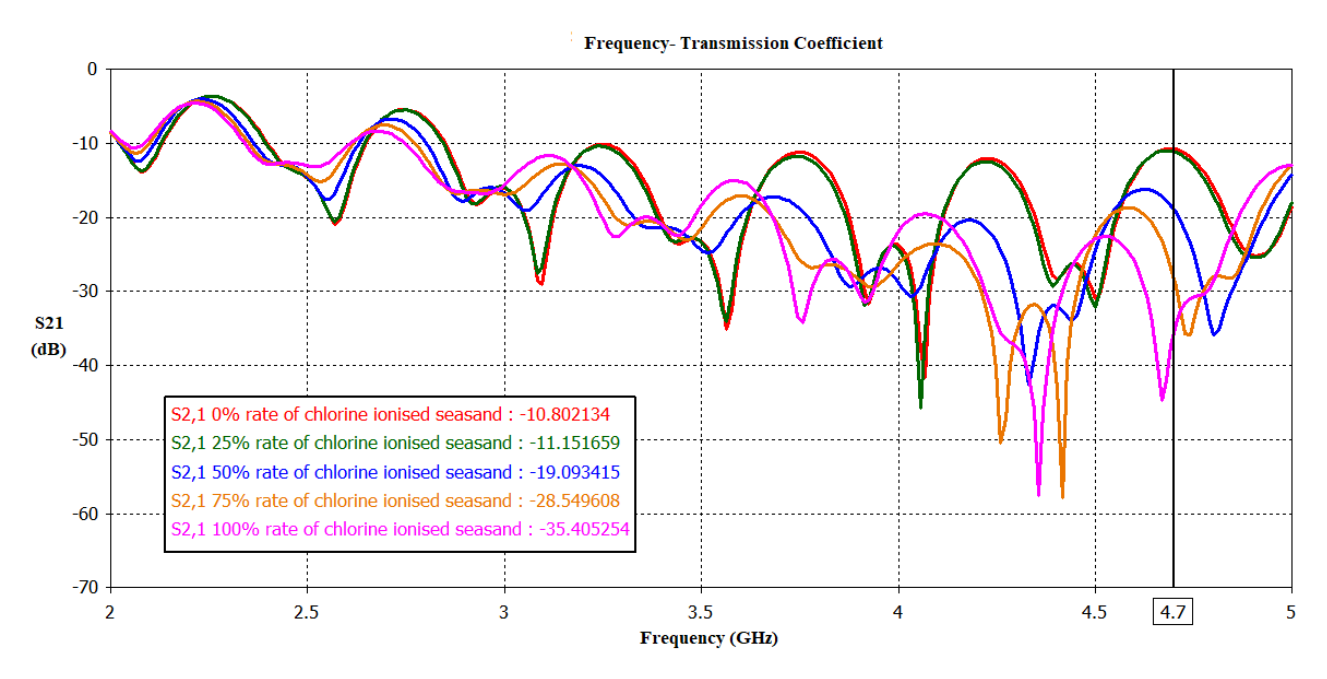


Figure 11. Simulation results and transmission coefficient results (S12) results with various contents for fourth structure.

3.3. Experimental Processes and Analyses

We can gain the relative permittivity values from the scattering parameters (that known as S11- S12- S21- S22 parameters). These parameters defined between the ports that show the reflected and transmitted electromagnetic signals.

One port and two-port system are considered in the study. Sparameters can be obtained and measured by using a network analyzer within the operating frequency range of analyzer. The measurement results of transmission/reflection coefficients (S21/S11) are shown in Figures 12-14. Four structures were fabricated with the help of the LPKF-E33 Circuit Printer.

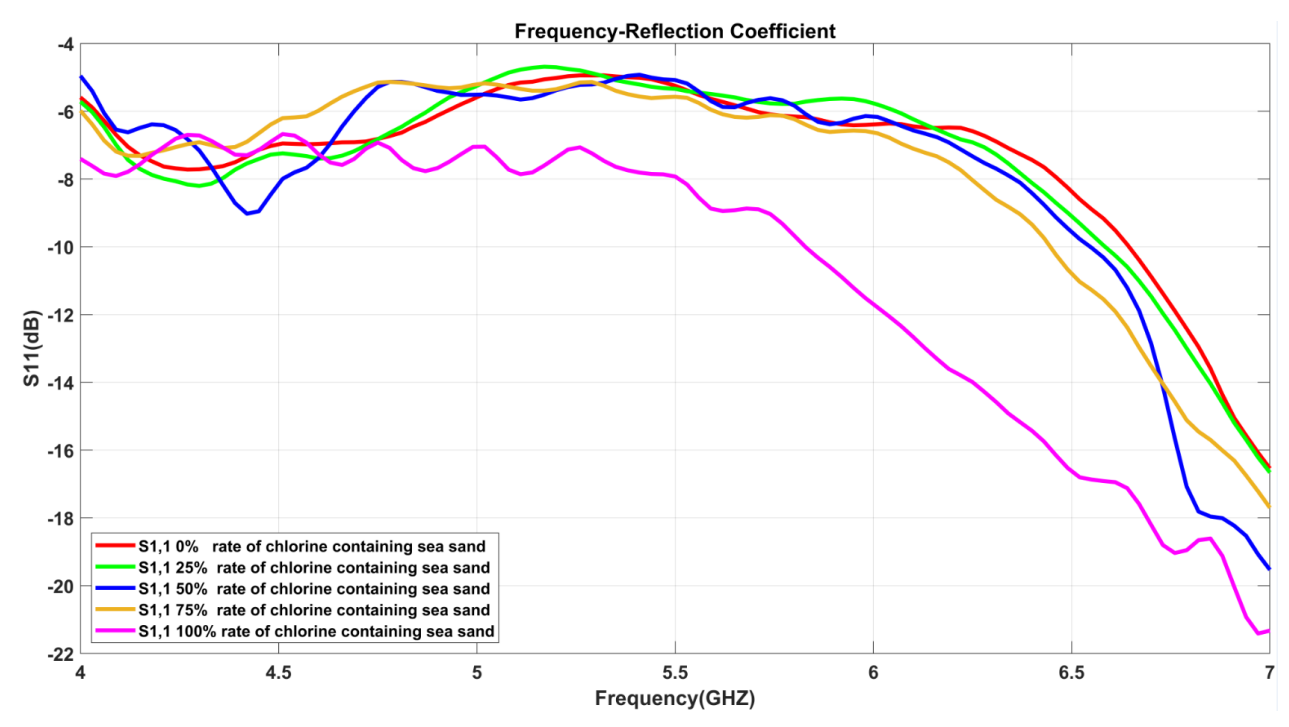


Figure 12. Value of reflection coefficient in loop like shape structure.

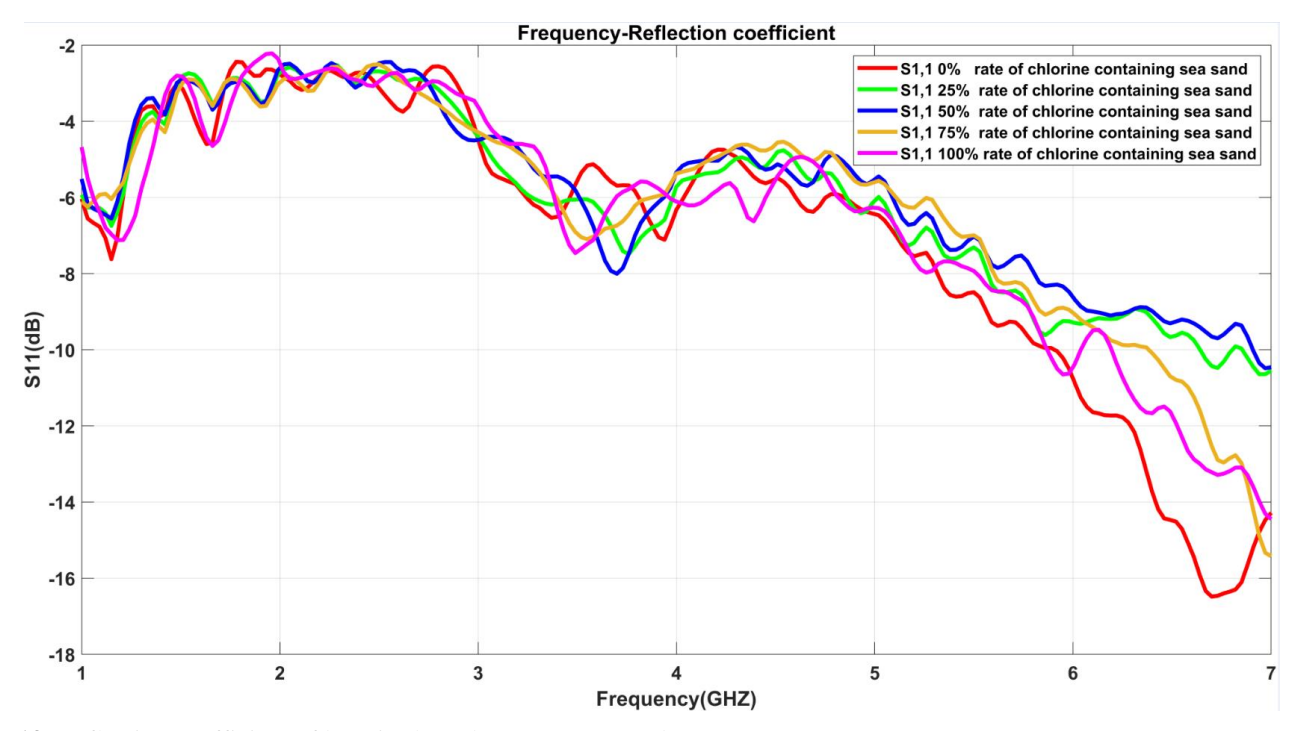


Figure 13. Reflection coefficient of bowtie shaped structure (second structure).

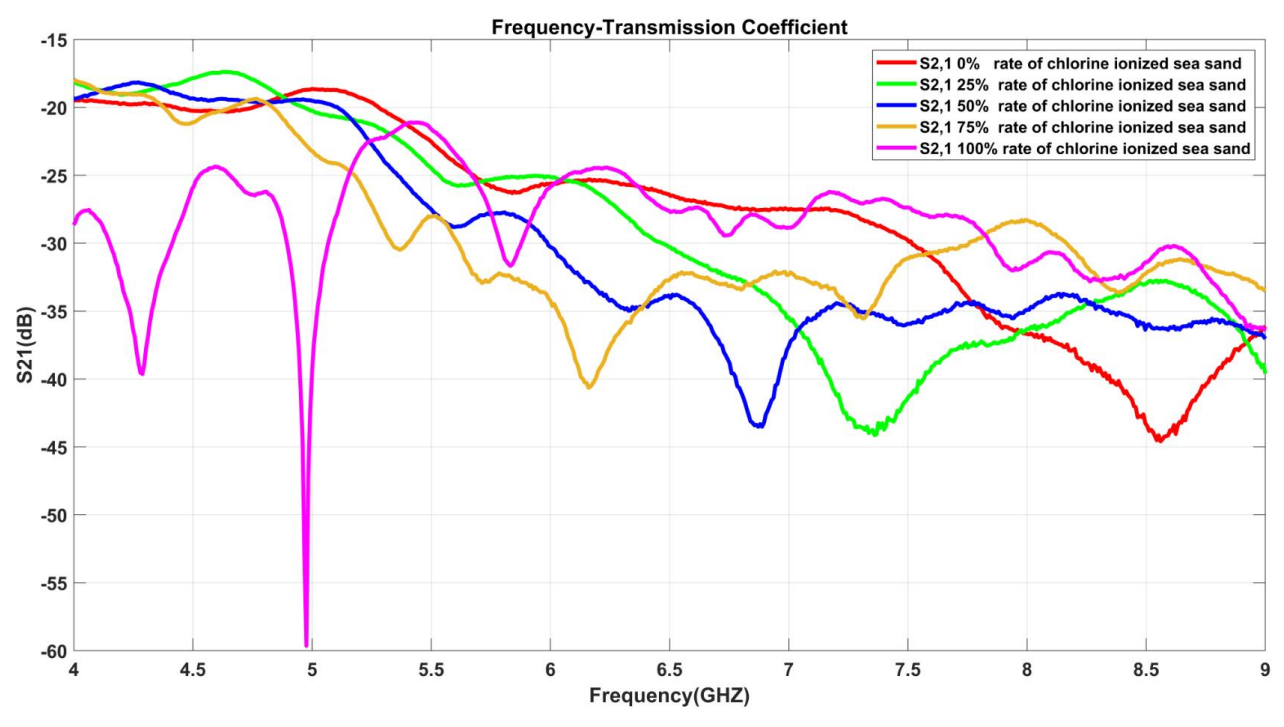


Figure 14. Transmission coefficient of double loop shaped (third structure).

We also created solder points for a feed line from the connectors to the antennas, as shown in Figures 15 and 16. There is regularity and linear array between transmissionresonance frequency graph and dielectric coefficient graph shown in Figure 7, 11, and 17. It can be seen that by increasing the rate of ionized sea sand between the 4 GHz and 5 GHz of frequency band, while the dielectric values in Figure 7 increase between this frequency range, the transmission coefficient values in Figures 11 and 17 decrease. Linearity can be explained with relation between dielectric constant and resonance frequency in sensor studies. In other words, the changing dielectric constant due to the increase or decrease of the capacitance or inductance effect causes continuous increase or decrease in resonance frequency. Resonance frequency of the whole system will change when the dielectric constants of the concrete samples changes. Since the parameter of chlorine sea sand changes the dielectric coefficient, the resonance frequency of the system will change. By comparing the changes in the reflection coefficient (S_{11}) with the dielectric constants of the samples, it can be seen these changes are in linear form. The results obtained from the simulation studies for the Structure with two Loop-like Antennas are evaluated and discussed with the experimental results in Figures 7, 10, and 14. As the proportion of ionized sea sand increases in concrete samples, the dielectric values in Figure 7 increase, while the transmission coefficient values in Figures 10 and 14 shift backwards. It can be seen that the experimental and numerical results are compatible with each other and there is little difference between them. These differences are due to manufacturing, calibration and materials.

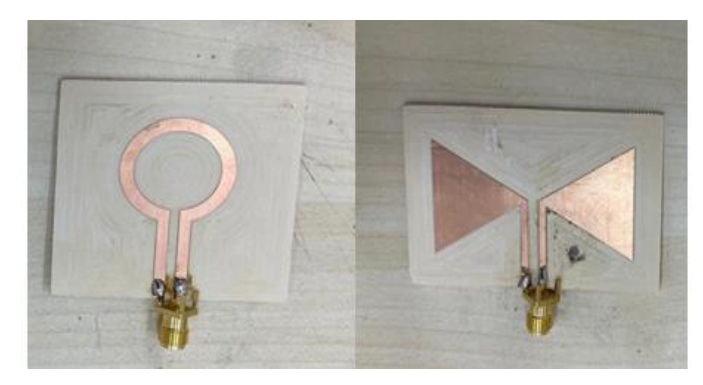


Figure 15. Fabrication of loop-like and bowtie shaped structure.

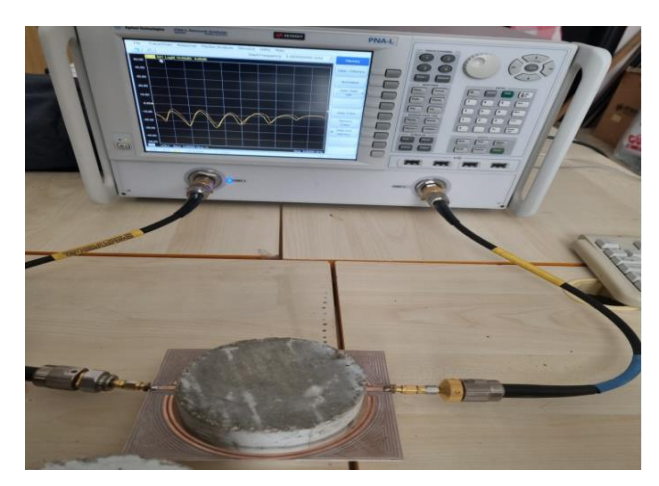


Figure 16. Experimental setup for fourth structure.

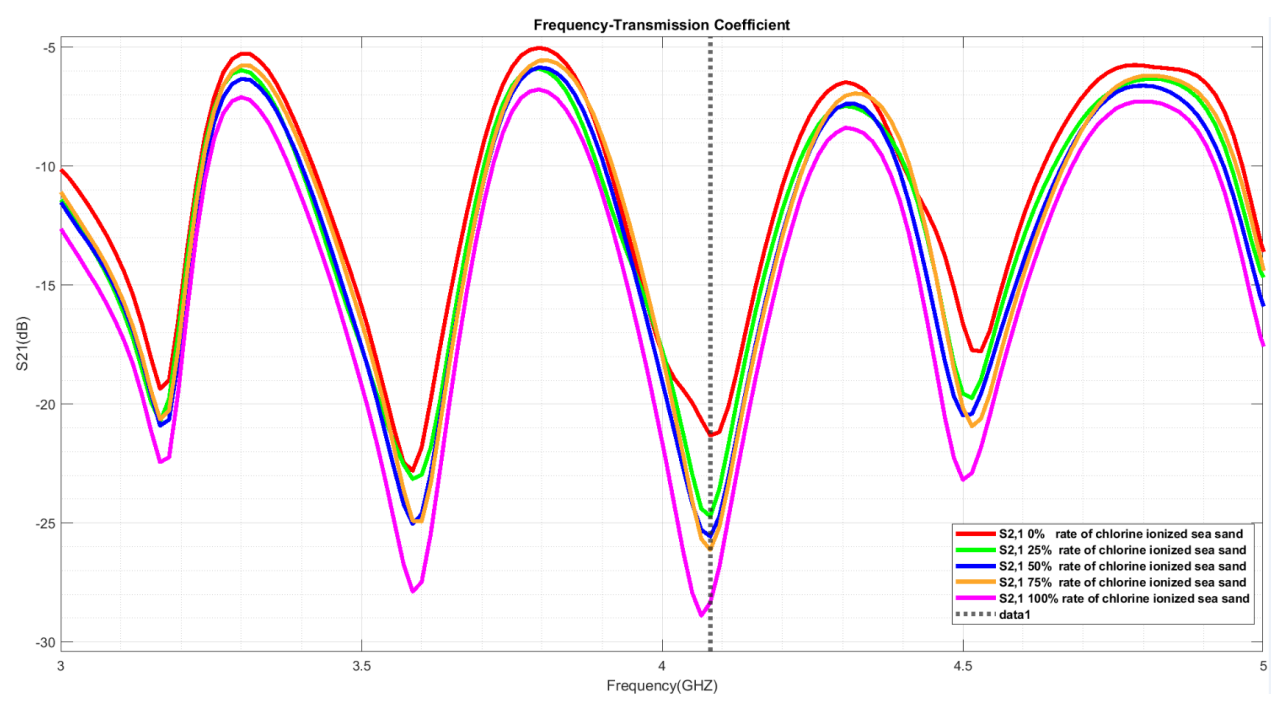


Figure 17. Transmission coefficient values of fourth structure.

4. Discussion

Fabricated antennas were fastened to probe of measuring device with electronic testers to measure radio frequency (RF) signals in an electronic circuit. Before experimental investigation, most of the devices as well as the vector network analyzer should be calibrated to obtain more accurate results at this step. In the experimental studies, the proposed structures are firstly fabricated and then samples are placed. After these processes the reflection, transmission coefficient and resonance frequency of structures are measured by using a vector network analyzer. The relationship between S parameters in concrete and dielectric constant of concrete are also investigated. Finally, the numerical and experimental results are compared to each other. We found the relationship between the obtained data after measuring the transmission/reflection (S12/S11) values. The results obtained from experimental study should verify the simulation study results.

5. Conclusion

Cracks in concrete or concrete with low resistance have many risks and in order to prevent the fall of structures, buildings and other damages, research on concrete is necessary. As can be observed from the minimum points in frequency band of structures, the higher content of chloride ionized sea sand has been decreased the transmission/reflection response of the sample due to reduced electromagnetic properties of the samples with increased di-electricity for incident wave. According to the results of the measurements, it has been observed that there is a linear resonance displacement among the different composites. The dielectric constant values for each material under test (MUT) are evaluated from the values of

reflection and transmission in the mentioned frequency range. As mentioned earlier, the corrosion process of materials such as stone or concrete can occur in building materials and unfortunately cause damage or injury or physical harm. This is due to ionized sand particles, especially chlorine ions. These proposed constructs and models have the ability to appreciate and respond to complex influences, sensitivity and they are so economical, inexpensive and not difficult to manufacture.

Acknowledgment

The authors would like to thank Physics Department of Çukurova University and Electrical and Electronics Engineering Department of Iskenderun Technical University for providing any support and for the opportunity to publish this work.

Conflict of Interest

The authors declare that they have no conflict of interest.

References

Abbas, Z., Yeow, Y. K., Shaari, A. H., Khalid, K., Hasan, J., & Saion, E. (2005). Complex permittivity and moisture measurements of oil palm fruits using an open-ended coaxial sensor. *IEEE Sensors Journal*, *5*(6), 1281-1287. https://doi.org/10.1109/JSEN.2005.859249

Abdulkarim, Y. L., Deng, L., Karaaslan, M., & Unal, E. (2019). Determination of the liquid chemicals depending on the electrical characteristics by using metamaterial absorber based sensor. *Chemical Physics Letters*, 732, 136655. https://doi.org/10.1016/j.cplett.2019.136655

- Akgol, O., & Unal, H. (2018). Metamaterial-based multifunctional sensor design for moisture, concrete aging and ethanol density sensing applications. *Modern Physics Letters B*, 32(23), 1850271. https://doi.org/10.1142/S0217984918502718
- Bakır, M. (2017). Electromagnetic-based microfluidic sensor applications. *Journal of The Electrochemical Society*, 164(9), B488-B494. https://doi.org/10.1149/2.0171712jes
- Bakır, M., Karaaslan, M., Altıntaş, O., Bagmancı, M., Akdogan, V., & Temurtaş, F. (2018a). Tunable energy harvesting on UHF bands especially for GSM frequencies. *International Journal of Microwave and Wireless Technologies*, 10(1), 67-76. https://doi.org/10.1017/S1759078717001325
- Bakır, M., Karaaslan, M., Unal, E., Akgol, O., & Sabah, C. (2018b). Sensory applications of resonator based metamaterial absorber. *International Journal of Light and Electron Optics*, 168(18), 741-746. https://doi.org/10.1016/j.ijleo.2018.05.002
- Bakır, M., Dalgaç, Ş., Karaaslan, M., Karadağ, F., Akgol, O., Depci, T., & Sabah, C. (2019). A Comprehensive study on fuel adulteration sensing by using triple ring resonator type metamaterial. *Journal of The Electrochemical Society*, *166*(12), B1044. https://doi.org/10.1149/2.1491912jes
- Cai, W., Chettiar, U. K., Kildishev, A. V., & Shalaev, V. M. (2007). Optical cloaking with metamaterials. *Nature Photonics*, 1(4), 224-227. https://doi.org/10.1038/nphoton.2007.28
- Chieh-Sen, L., & Yang, C. L. (2014). Thickness and permittivity measurement in multi-layered dielectric structures using complementary split-ring resonators. *IEEE Sensors Journal*, 14(3), 695-700. https://doi.org/10.1109/JSEN.2013.2285918
- Ebrahimi, A., Withayachumnankul, W., Al-Sarawi, S., & Abbott, D. (2014). High-sensitivity metamaterial-inspired sensor for microfluidic dielectric characterization. *IEEE Sensors Journal*, *14*(5), 1345-1351. https://doi.org/10.1109/JSEN.2013.2295312
- Liu, Y., Zhou, X., Song, K., Wang, M., & Zhao, X. (2015). Ultrathin planar chiral metasurface for controlling gradient phase discontinuities of circularly polarized waves. *Journal of Physics D: Applied Physics*, 48(36), 365301. https://doi.org/10.1088/0022-3727/48/36/365301

- Pendry, J. B., Holden, A. J., Stewart, W. J., & Young, I. (1996). Extremely low frequency plasmons in metallic mesostructures. *Physical Review Letters*, 76(25), 4773-4776. https://doi.org/10.1103/PhysRevLett.76.4773
- Pendry, J. B., Holden, A. J., Robbins, D. J., & Stewart, W. J. (1999). Magnetism from conductors and enhanced nonlinear phenomena. *IEEE Transactions on Microwave Theory and Techniques*, 47(11), 2075-2084. https://doi.org/10.1109/22.798002
- Plum, E., Zhou, J., Dong, J., Fedotov, V. A., Koschny, T., Soukoulis, C. M., & Zheludev, N. I. (2009). Metamaterial with negative index due to chirality. *Physical Review B*, 79(3), 035407. https://doi.org/10.1103/PhysRevB.79.035407
- Smith, D. R., Padilla, W. J., Vier, D. C., Nemat-Nasser, S. C., & Schultz, S. (2000). Composite medium with simultaneously negative permeability and permittivity. *Physical Review Letters*, 84(18), 4184-4187. https://doi.org/10.1103/PhysRevLett.84.4184
- Veselago, V. G. (1968). The electrodynamics of substances with simultaneously negative values of ϵ and μ . *Soviet Physics Uspekhi*, 10(4), 509-514. https://doi.org/10.1070/PU1968v010n04ABEH003699
- Yang, L., Bowler, N., & Johnson, D. B. (2011). A resonant microwave patch sensor for detection of layer thickness or permittivity variations in multilayered dielectric structures. *IEEE Sensors Journal*, 11(1), 5-15. https://doi.org/10.1109/JSEN.2010.2051223
- Yang, C. L., Lee, C. S., Chen, K. W., & Chen, K. Z. (2016). Noncontact measurement of complex permittivity and thickness by using planar resonators. *IEEE Transactions* on *Microwave Theory and Techniques*, 64(1), 247-257. https://doi.org/10.1109/TMTT.2015.2503764
- Zhang, S., Park, Y. S., Li, J., Lu, X., Zhang, W., & Zhang, X. (2009). Negative refractive index in chiral metamaterials. *Physical Review Letters*, 102(2), 023901. https://doi.org/10.1103/PhysRevLett.102.023901
- Zile, M. (2019). Temperature analysis in power transformer windings using created artificial bee algorithm and computer program. *IEEE Access*, 7(3), 60513-60521. https://doi.org/10.1109/ACCESS.2019.2915343